

# Towards nanometer accuracy laser metrology for phase-referenced interferometry with the VLTI

Samuel Lévêque<sup>a</sup>, Rainer Wilhelm<sup>a</sup>,  
Yves Salvadé<sup>b</sup>, Olivier Scherler<sup>b</sup>, René Dändliker<sup>b</sup>

<sup>a</sup>European Southern Observatory (ESO), Garching bei München, Germany<sup>‡</sup>

<sup>b</sup>Institute of Microtechnology (IMT), Neuchâtel, Switzerland

## ABSTRACT

The PRIMA laser metrology system is being developed to monitor optical path differences and optical path fluctuations encountered by two stellar objects inside the VLTI during phased-referenced observations. This system, which will operate at the scale of the VLTI, has an accuracy goal of a few nanometers. After an introduction to its design, based on heterodyne interferometry, this paper presents the results of sub-system characterization and prototyping as well as experimental results obtained during full-scale testing at the Paranal Observatory.

**Keywords:** Laser metrology, interferometry, stellar interferometry, Very Large Telescope Interferometer (VLTI)

## 1. INTRODUCTION

Forthcoming phase-referenced interferometric programs with the VLTI are targeted towards the detection of extra-solar planets as well as high-resolution imaging of faint stars<sup>1</sup>. This technique relies on the simultaneous observation of the interference fringes produced by two stellar objects. In the VLTI, the light captured by two telescopes follows a train of 25 mirrors distributed along a subterranean path of approximately 200 meters, before being coherently combined. The fringe signals are affected by static optical path differences and by time-varying optical path fluctuations due to vibrations of mechanical structures, air turbulence inside the interferometer and delay line motion. A laser metrology system is currently designed to monitor these instrumental disturbances with an accuracy goal of 5 nm.

The concept of the PRIMA metrology system developed by ESO in collaboration with the Institute of Microtechnology of Neuchâtel (IMT) is based on “super-heterodyne laser interferometry”, where two heterodyne Michelson interferometers are operating simultaneously and have common optical paths with both observed stars through the VLTI optical train<sup>2</sup> (see Figure 1). The disturbance to be monitored,  $\Delta L$ , corresponds to the difference between the path variations recorded by the two Michelson interferometers. Each interferometer arm length reaches up to 552 m (return way), with an optical path difference of 120 m, varying at a maximum speed of about  $25 \text{ mm s}^{-1}$ . The two interferometers use different heterodyne frequencies (650 kHz and 450 kHz) to possibly suppress any crosstalk signals. These frequencies are generated using four fiber-coupled acousto-optics modulators connected to a single Nd-YAG laser. After photodetection and filtering, the individual heterodyne signals are mixed such that the disturbance to be monitored is directly coded in the phase of a 200 kHz carrier signal (i.e.  $650 \text{ kHz} - 450 \text{ kHz}$ ). All band-pass filters are designed to minimize any differential phase shift in the detection band. This super-heterodyne detection is tailored to our operating conditions. Indeed the disturbance  $\Delta L$  has a low amplitude and bandwidth compared to the individual optical path differences occurring in each interferometer. This is a consequence of having two interferometers with a large path in common. Super-heterodyne detection avoids the need for two independent high bandwidth and highly synchronized phase measurements. The band-

---

<sup>‡</sup> Email: sleveque@eso.org, URL: <http://www.eso.org/projects/vlti>

width of the phase meter is rather used for phase averaging to possibly increase the overall system accuracy. Finally, the phase of the 200 kHz carrier signal is measured based on the principle of time interval measurement using a 200 MHz clock signal. It involves programmable logic components of the *Altera Max7000B* family. In order to minimize instrumental phase shifts, the clock signal is derived from the 200 kHz interferometric reference signal using a phase lock-loop. The measured phase can be averaged over a user-defined integration time ranging from 20  $\mu$ s to 0.65 s. All components, including the fiber-pigtailed photo-detectors are mounted on VME-boards.

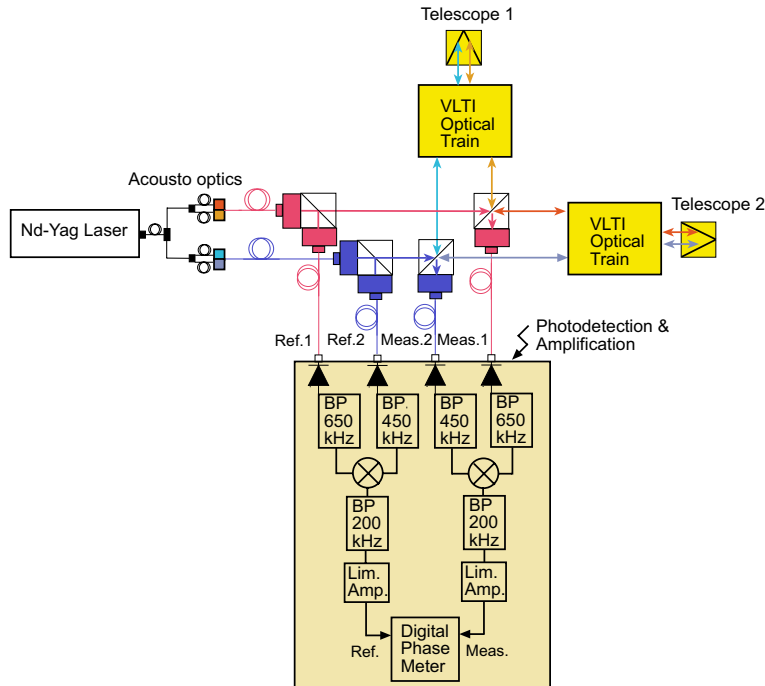


Fig. 1: Sketch of the laser interferometer's configuration

## 2. CHARACTERIZATION OF THE LASER AND OF THE ACOUSTO-OPTICS MODULATORS

### 2.1 Selection of the laser head

The selection of the laser head was based on several criteria. Its wavelength,  $\lambda$ , must lie both outside the sensitivity region of Silicon detectors used by the adaptive optics system of the VLT1 as well as outside the H, K and N-Bands used by the scientific instruments associated with PRIMA. In addition, its coherence length must be much larger than 240 m, corresponding to the maximum optical path difference in each PRIMA channel. Also, an optical power P larger than 100 mW must be available considering our operating conditions.

Finally, the laser frequency,  $\nu = c/\lambda$ , must be sufficiently stable such that the corresponding optical path difference (OPD) error is less than 1 nm over a differential internal OPD of  $\Delta L = 100$  mm. This corresponds to a frequency stability of better than  $10^{-8}$ , which in the case of PRIMA observations applies to a time window ranging from 125  $\mu$ sec to 30 minutes. In addition, the absolute value of the emitted laser frequency must be known with the same accuracy level during the lifetime of the metrology system to precisely convert the phase measurements into OPD values.

Based on the above requirements and constrains, we have selected a Nd-YAG laser emitting at 1319 nm (*Lightwave Electronics Model 125*). This type of "Non Planar Ring Oscillator" (NPRO) laser<sup>†</sup> provides an intrinsic narrow line width

and good frequency stability as well as sufficient optical power ( $P > 200$  mW). The laser frequency can be slowly tuned by changing the NPRO's temperature (typically  $-2.4$  GHz/ $^{\circ}$ C) or for a higher bandwidth by applying a stress on the crystal using a piezo actuator (typically 1 MHz/V).

## 2.2 Characterization of the frequency spectrum

We have characterized the spectrum of the Nd-YAG laser as shown in Figure 2. In order to bring out the secondary emissions lines, the main lasing wavelength of  $\lambda = 1319$  nm was attenuated by a density of 6, using a holographic notch filter. The strongest component is generated by the pump diode emitting at 810 nm. It has a relative intensity of  $2.3e^{-9}$  with respect to  $\lambda$ . However, only the components 1339 nm, 1357 nm and 1414 nm are actually transmitted through the fiber-pigtailed acousto-optics modulators and relayed in the VLTI optical train. These components are taken into account in the straylight analysis of the PRIMA laser metrology.

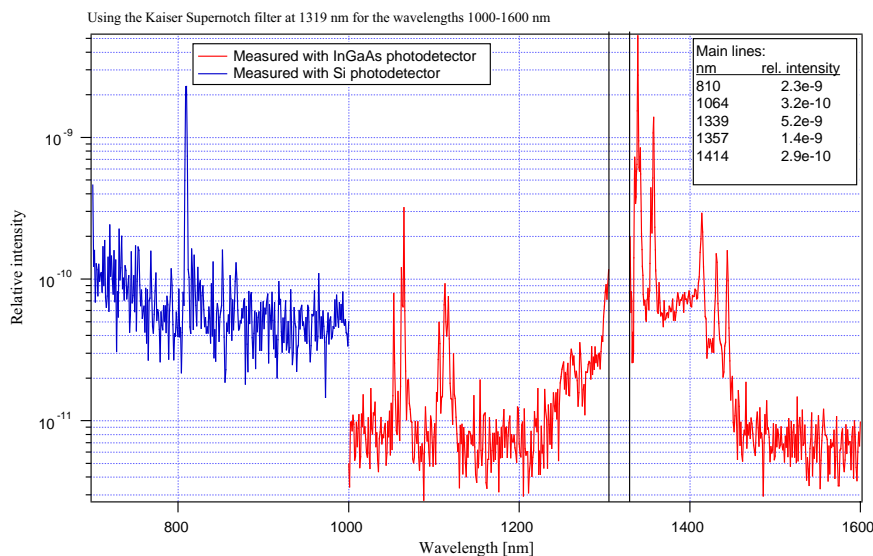


Fig. 2: Measured spectrum of the Nd-YAG laser; the main emission line ( $\lambda = 1319$  nm) has been suppressed using a holographic notch filter to highlight the secondary emission lines.

## 2.3 Characterization of the frequency stability

The frequency stability of the laser was estimated by measuring the beat frequency generated by two identical free running Nd-YAG lasers, over a period of one hour. Assuming that the frequency noise of the two lasers is not correlated, the contribution of one laser is given by applying a factor  $\sqrt{2}$  to the measured beat frequency. The results are reported in Figure 3. The results showed that the power spectral density (PSD) of the laser frequency fluctuations can be fitted by the function:

$$\text{PSD}_{\text{dv}} = 10^{10} \times f^{-2} \text{ (in Hz}^2 \text{ per Hz, for } f < 10 \text{ kHz)}$$

These results are in good agreement with previous measurements<sup>3</sup>. For an observation time of 30 minutes, the associated standard deviation of the OPD fluctuations is about 9 nm per meter of OPD. In the next months, we will implement an absolute frequency stabilization scheme based on second harmonic generation and frequency locking on a Iodine cell<sup>4</sup>.

‡ Also available from other suppliers

In the meantime, we stabilized the beat frequency of the two lasers by acting on both the temperature and the piezo actuator of one laser, to possibly determine the accuracy of the phase meter as explained in Section 3. The lower part of Figure 3 shows that the remaining fluctuations of the beat frequency reached a level of about  $10^5 \text{ Hz}/\sqrt{\text{Hz}}$ .

Finally, the laser head was used in a fiber Mach-Zehnder interferometer, where the OPD was 1.5 km. The contrast of the interference signal indicated that the coherence length of the laser was larger than 1.5 km which is sufficient for our application.

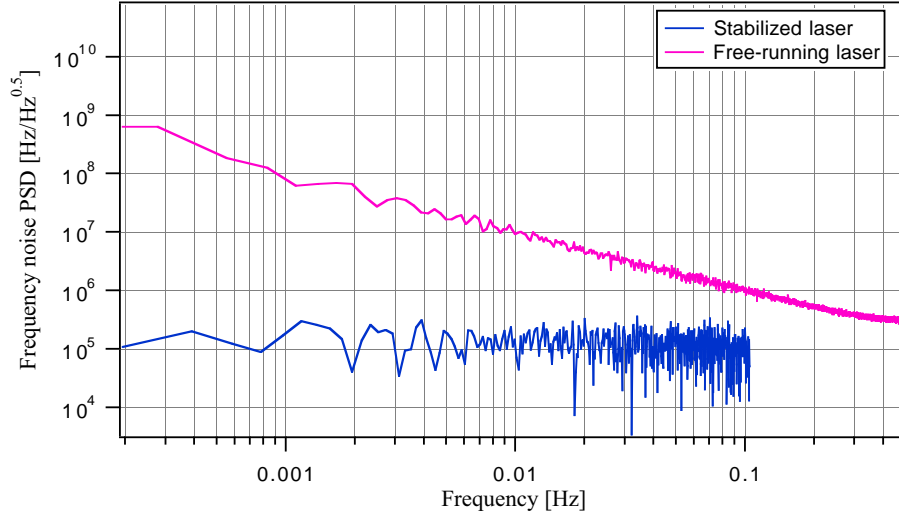


Fig. 3: Frequency noise of the free running Nd-YAG laser (upper line) and after relative stabilization to another similar Nd-YAG laser (lower line).

#### 2.4 Fiber-pigtailed acousto-optics modulators

In order to generate the appropriate heterodyne frequencies, the laser head output is split into four beams using three cascaded Single Mode and Polarization Maintaining (SM-PM) fiber couplers. These four linearly polarized laser outputs are connected to four fiber-pigtailed and polarization maintaining Acousto-optics modulators (*IntraAction series FCM-40*), which generate four frequency shifted laser components (see Figure 4). For the first interferometric channel, the generated frequencies are  $\nu + 38 \text{ MHz}$  and  $\nu + 38.65 \text{ MHz}$ . The corresponding heterodyne frequency is  $f_1 = 650 \text{ kHz}$ . For the second interferometric channel, the generated frequencies are  $\nu - 40 \text{ MHz}$  and  $\nu - 39.55 \text{ MHz}$ , corresponding to an heterodyne frequency  $f_2 = 450 \text{ kHz}$ . In the worst case, the measured transmission factor from the laser to the output of any of the four acousto-optics modulators was at least 8.7%. We intend to replace the current couplers by fusion spliced fiber couplers to improve the overall transmission. These couplers will also be temperature controlled to eliminate any intensity modulation known to occur in cascaded PM components.

### 3. PHASE METER PROTOTYPE

A prototype of the overall photo-detection and phase measurement chain has been built at IMT. The performance of this system was evaluated to demonstrate the ability to achieve a 5 nm accuracy, but—in a first phase—independently from the VLTI environment.

The results showed that the fiber-pigtailed photo-detectors offer a Noise Equivalent Power (NEP) of  $0.2 \text{ pW}/\sqrt{\text{Hz}}$  and a bandwidth of 10 MHz. The NEP is actually very close to the Johnson noise limit of  $0.15 \text{ pW}/\sqrt{\text{Hz}}$ , given by the load resistor of the photodiode at a temperature of  $20^\circ\text{C}$ .

The resolution of the digital phase meter board is  $2\pi/1024$  (or 0.64 nm in double pass) with a maximum sampling frequency of 200 kHz. The standard deviation of the phase noise is less than  $2\pi/1024$ , for an optical power higher than 100 nW per interferometric arm and a fringe contrast of 70%.

For the same fringe contrast, the measured accuracy was  $2\pi/800$  (or 0.8 nm in double pass) for a 50 kHz bandwidth and a photodetected power of 20 nW per interferometric arm. Testing a phase accuracy performance at the  $2\pi/1000$  level is actually a very difficult task in laboratory conditions since it requires an equivalent mechanical and environmental stability. Our approach was to take advantage of two-wavelength interferometry, where the phase accuracy is measured on a synthetic wavelength much larger than the optical wavelength. We used two Nd-YAG lasers operating with a frequency difference of 1.5 GHz to generate a synthetic wavelength of 200 nm. In this case, we only needed to introduce a path variation known with a 0.1 mm accuracy to demonstrate a system accuracy of  $2\pi/1000$ . The frequency difference of the two lasers was stabilized at the  $5 \cdot 10^{-5}$  level by monitoring the 1.5 GHz beat frequency and by controlling accordingly the length and temperature of the cavity of one of the two lasers.

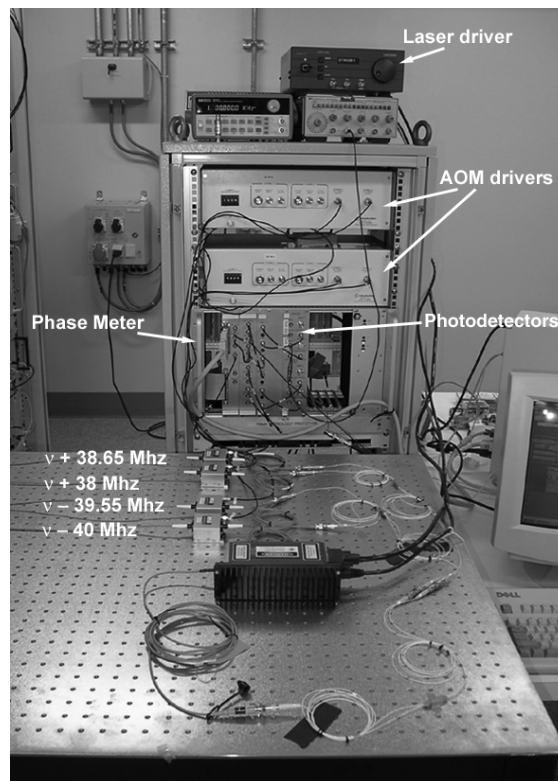


Fig. 4: Picture of the laser head, the fiber couplers and acousto-optics modulators. This view includes the prototype VME boards containing the photodetectors, the signal conditioning electronics and the phase meter.

## 4. PROTOTYPE TESTING AT PARANAL

### 4.1 Objectives

In April 2002, a complete prototype of the PRIMA metrology system was tested at Paranal. The objective of this test campaign was to characterize the behaviour of the metrology system under representative operating conditions by analyzing the impact of the VLTI optical train, of the internal environmental conditions, and of the propagation length. More precisely, the tasks performed during the test campaign were:

- Quantification of the impact of the VLTI optical train on the polarization state of the PRIMA metrology beams as well as its polarization-dependent transmission at the laser wavelength  $\lambda = 1319$  nm
- Quantification of the frequency spectrum of internal optical path difference (OPD) fluctuations and identification of their origin
- Measurement of the contrast of the interference signal obtained after full propagation inside the VLTI
- Measurement of both image and lateral pupil motion of the laser beams
- Evaluation of the performance of hardware components (e.g. opto-mechanics for beam injection into the stellar path, beam combiner) and identification of potential interface problems between the PRIMA metrology and the VLTI



*Fig. 5: Beam path followed by the laser beams during the test campaign at Paranal; it included all mirrors of the VLTI optical train up to the Nasmyth focus of UT1 and UT3. The maximum optical path length was 520 m (return way). The white circle indicates the location of the interferometric laboratory where the metrology beams were injected into the stellar paths.*

### 4.2 Experimental setup

Using four 35 m SM-PM fibers, the four frequency shifted laser beams generated by the acousto-optics modulators shown in Figure 4 were relayed towards the VLTI interferometric laboratory. This electronic equipment was located in a separate room. In this way, neither vibrations nor power dissipation was transferred into the interferometric laboratory. Each pair of fibers was connected to a beam combiner assembly as shown in Figure 6 (left) for the “v + 38 MHz” and “v + 38.65 MHz” fibers. For each beam combiner assembly the two incoming beams are connected to a fiber-pigtailed collimator whose orientation defines two orthogonal states of linear polarization “s” and “p”. These incoming “s” and “p” components are first superimposed on a polarizing beam splitter (PBS). On one hand, the polarization leakage of the PBS cube is used to generate a 650 kHz interference signal between the “s” and “p” components (respectively 450 kHz for the

second beam combiner). The phase of this reference signal is a measurement of all phase variations that occurred along the 35 m fiber relay. The reference signal is injected into a 35 m multimode fiber which is connected to one of the four photodetectors of the phase meter.

On the other hand, almost all the power of the “s” and “p” components is directed towards a non-polarizing beam splitter (BS). Although both polarizations are equally reflected and transmitted, an additional linear polarizer located on both the reflected and the transmitted side of the BS allows to select only one polarization state (“p” or “s”). Thus, the “s” and “p” components are physically separated in two different interferometric arms. This configuration corresponds to a standard polarizing heterodyne interferometer. The “s” and “p” components are injected into two different 5 m SM-PM fibers which are connected to “fiber collimators”. Then each metrology beam is collimated into a 10 mm diameter beam and is injected either into the UT1 interferometer arm or into the UT3 arm. Figure 6 (right) shows how the  $\nu - 40$  MHz and  $\nu + 39.55$  MHz signals are injected into the VLTI optical train using two fiber collimators, mounted on two 5-axis stages.

Starting from an initial laser optical power of 220 mW, the optical power of each metrology component finally injected into each VLTI arm was about 3 mW. This corresponds to a transmission of 1.4%.

After a round trip through the VLTI, including the Nasmyth mirror of UT1 or UT3, the retro-reflected laser beams are superimposed on the BS of their respective beam combiner assembly to generate the interference “probe” signals ( $f_1 = 650$  kHz for the VINCI Channel and  $f_2 = 450$  kHz for the MIDI Channel<sup>‡</sup>). The probe signals are injected into a 35 m multi-mode fiber (as for the reference signals described above) and are detected by two independent photodetectors of the phase meter which is located in a separate room. Because the PRIMA star separators are not yet available on the Unit Telescopes, it was not possible to propagate the metrology beams inside the VLTI optical train in two physically separated channels (i.e., four interferometric arms), as it will be during “real” PRIMA operation<sup>2</sup>. Therefore, the two metrology channels were superimposed on two beam splitters, as shown in Figure 6 (right). Thus, any OPD variations occurring between these beam splitters and the telescopes were common to both channels. This configuration actually simulates the case when the star separators will be in calibration mode, i.e. when a full “cross-talk” appears between the two metrology channels.

During the polarization measurements, only the optical beam noted “-39.55 MHz” in Figure 6 was actually used. After collimation in free space, three different states of polarization (linear vertical, linear horizontal, circular) were successively generated using dedicated wave plates. The laser beam propagated up to the Nasmyth focus of UT3 after bouncing on 19 surfaces, including one dichroic mirror, and propagated back through the beam splitter shown in Figure 6 (right) where it was analyzed using a linear polarizer and a photodetector.

---

<sup>‡</sup> The notations “MIDI” or “VINCI” refer to the two metrology channels. This is a convention used during the test period only. It is not related to the operation of these two VLTI instruments with PRIMA.

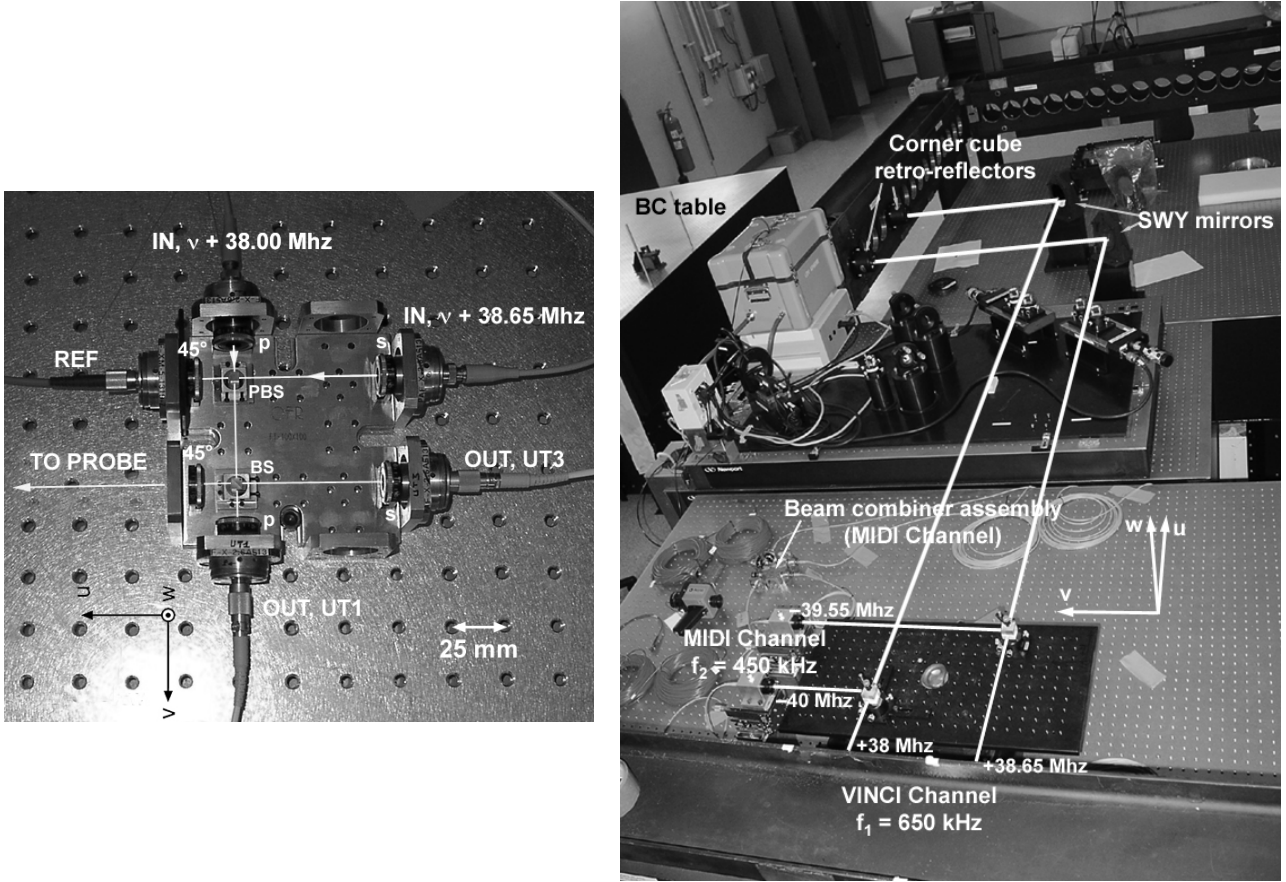


Fig. 6: **Left:** beam combiner assembly for the VINCI Channel interferometer (heterodyne frequency  $f_1 = 650$  kHz); The labels “s”, “p” and “45°” denote the orientation of the transmission axes of the polarizers. The edge of the beam splitter (BS) is 5 mm. The beam combiner assembly of the MIDI Channel is strictly identical. Both combiners were located inside the interferometric laboratory.  
**Right:** injection of the two pairs of interferometric beams (corresponding to the VINCI and MIDI Channels) into the VLTI optical train; The two beam combiner assemblies are located on the MIDI feeding optics table, (on the picture only one beam combiner assembly can be seen). The picture was taken during alignment when two corner cube retro-reflectors were interrupting the optical beams, which otherwise propagated to the telescopes during the measurement sequence.

### 4.3 Measurement results

#### 4.3.1 State of polarization

Table 1 summarizes the results of the polarization measurements. The state of polarization of the retro-reflected beam can be described by two intensity transmission coefficients  $T_{\text{VLTI}}^s = 17.1\%$  and  $T_{\text{VLTI}}^p = 19.4\%$  for two orthogonal input polarization directions and a phase shift  $\Delta\phi_{s-p} = 10.5^\circ$  between these two components. These results indicate that the overall VLTI optical train is compatible with the implementation of polarizing heterodyne interferometry. In particular, there is no risk that an injected linear polarization is flipped by  $90^\circ$  which would completely extinct the detected retro-reflected metrology beam. The slight “depolarization” of the injected signal from linear to elliptical only affects the amplitude of the detected signals but not the phase.



Table 1: Summary of polarization measurements for a round trip through the VLTI (up to the Nasmyth mirror of UT3) and a wavelength of  $\lambda = 1319 \text{ nm}$

Input state of polarization		Output state of polarization	
Linear, Vertical		Elliptical $T_{\text{VLTI}}^{\text{s}} = 17.1 \%$	
Orientation:	$90^\circ$	Orientation:	$94^\circ$
Ellipticity:	$0^\circ$	Ellipticity:	$7.21^\circ$
Linear, Horizontal		Elliptical $T_{\text{VLTI}}^{\text{p}} = 19.4 \%$	
Orientation:	$0^\circ$	Orientation:	$-6^\circ$
Ellipticity:	$0^\circ$	Ellipticity:	$6.10^\circ$
Circular		Elliptical	
		$\Delta\phi_{\text{s-p}} =$	$10.5^\circ$

### 4.3.2 Optical path difference between UT1 and UT3

Internal OPD fluctuations have been reliably measured between UT1 and UT3 using a single metrology channel (450 kHz or 650 kHz). The optical path in each interferometric arm reached up to 520 m (return way). We also successfully performed similar measurements during motion of the delay lines. As “by-products”, we characterized the overshoot of the delay lines in positioning mode (0.2%) and confirmed the presence of mechanical vibrations at 48 Hz, generated by electronic cabinets located inside the Coudé room of the telescopes.

Figure 7 shows an example of these fluctuations recorded during day-time, i.e. when we had access to the telescopes, as well as its corresponding amplitude spectral density. Low frequency OPD variations reached  $80 \mu\text{m}$  peak-to-valley (P-V) over 30 min, with a drift of about  $1 \mu\text{m s}^{-1}$ . They were mainly introduced by internal air turbulence along the VLTI optical train. Indeed, we simultaneously observed a temperature fluctuation of typically  $dT = 0.1^\circ\text{K}$ . Considering an optical path of 520 m, a dependence of the index of refraction of  $dn/dT = -10^{-6} \text{ K}^{-1}$  gives a theoretical shift in optical path of  $52 \mu\text{m}$ .

The level of OPD error introduced by the laser frequency noise is reported in Figure 7, based on the results presented in Section 2.3. The Signal-to-Noise Ratio, SNR, of the reference signal over the detection bandwidth of 50 kHz was 9600, i.e. 39.8 dB. This corresponds to a phase error of  $d\phi = \text{SNR}^{-1/2} = 1.02e^{-2}$  rad or 2.14 nm for  $\lambda = 1319 \text{ nm}$ . The probe signals contained some parasitic interferences leading to an estimated OPD error of 20 nm P-V. These parasitic interferences were introduced by polarization leakage, resulting from the limited extinction ratio of the polarizers that we have used and from the non-perfect perpendicularity of the superimposed “s” and “p” components. Like in any polarizing heterodyne interferometer, this cyclic error should have a period corresponding to an OPD fluctuation of  $\lambda/2$ . For the implementation of a polarized heterodyne metrology system for PRIMA, this error needs to be reduced by at least a factor 4. In this case, we need to use better polarization components and/or implement methods reported in the literature to average out polarization leakage errors<sup>5</sup>.

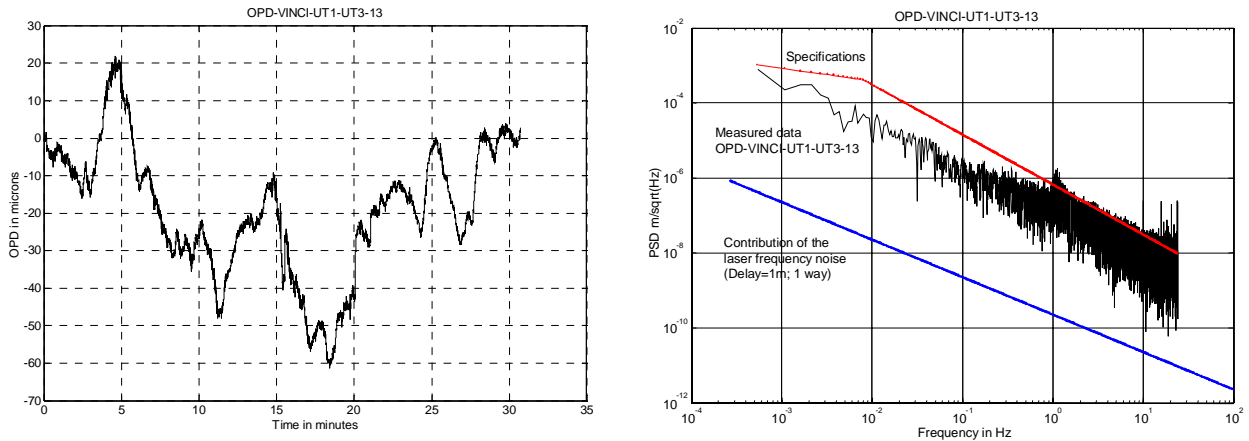


Fig. 7: **Left:** Temporal fluctuation of the OPD between UT1 and UT3 measured during day time with the 650 kHz heterodyne channel; the total optical path was about 520 m (return way). Both delay lines were fixed and positioned at 100 m. **Right:** Corresponding amplitude spectral density; the plot also shows the contribution of the laser frequency noise.

### 4.3.3 Differential optical path difference between the two metrology channels

By operating simultaneously both metrology channels, that is, by monitoring the phase of the 200 kHz super-heterodyne signal, we essentially checked the level of *differential* OPD fluctuations,  $\Delta L$ , occurring inside the VLTI laboratory. Indeed, as explained in Section 4.2, the two metrology channels essentially followed a common path while propagating towards the telescopes. During this measurement sequence, we verified that the displacement of the delay lines had no impact on the signal measured by the phase meter.

The amplitude of  $\Delta L$  reached a few microns over half an hour as shown in Figure 8. The main contribution originated from OPL fluctuations inside the optical fibers used to relay the metrology beams of each channel to each VLTI arm. These fibers (noted “OUT UT1” and “OUT UT3” in Figure 6) will not be used in the final configuration of the PRIMA metrology. Indeed, the laser beams will propagate in air after separation by the polarizing beam splitter of the beam combiner shown in Figure 6.

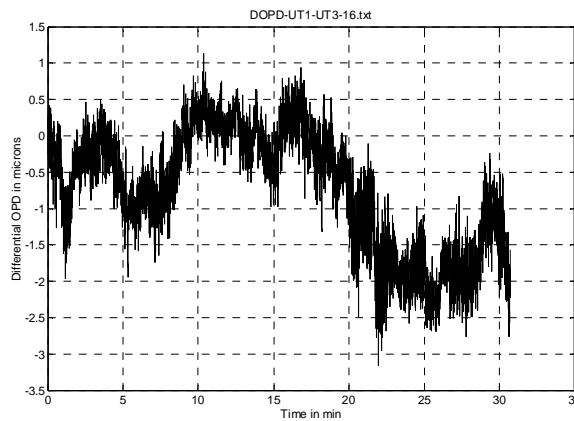


Fig. 8: Example of the differential optical path recorded between UT1 and UT3, along a 520m optical path (return way) and over 30 minutes.

#### 4.3.4 Fringe contrast and received optical power

The fringe contrast of the probe signals exceeded 80%, after a round-trip through the VLTI, including spatial filtering by the injection fibers. Its standard deviation was about 5%. The contrast was estimated by undersampling the optical power,  $P$ , of the 650kHz (or the 450 kHz) interferometric probe signal at 1kHz and by computing  $(P_{\max}-P_{\min})/(P_{\max}+P_{\min})$  over a time window of 100 samples (i.e 0.1 s). An example of the results is plotted in Figure 9.

The ratio of the mean optical power re-coupled into the SM fibers divided by its standard deviation reached a maximum value of 19 (see Figure 9). This value also includes remaining alignment errors, tilt and lateral pupil motion due to internal seeing (see Section 4.3.5).

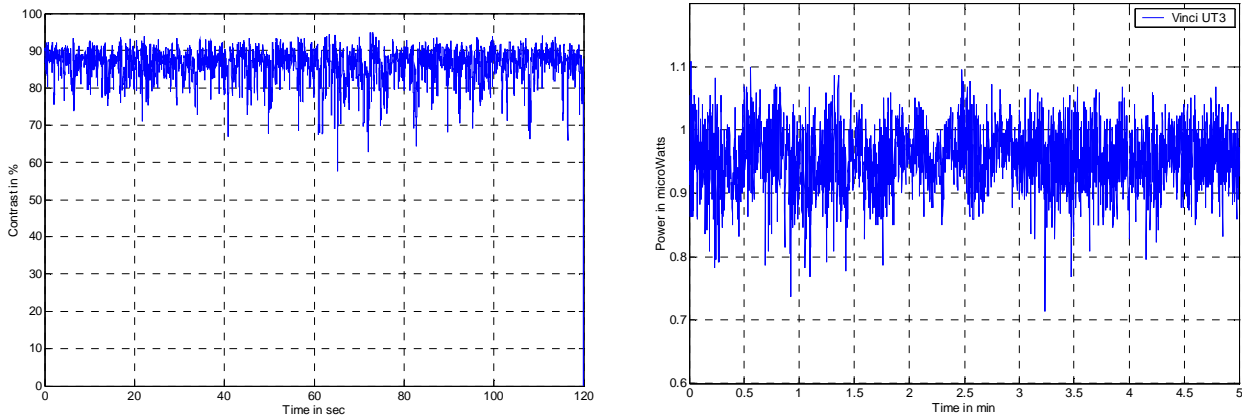


Fig. 9: **Left:** Fringe contrast of the probe interference signal of the MIDI channel during measurements between UT1 and UT3  
**Right:** Power re-coupled into a SM fiber over a 5 min period after a round trip up to UT3  
Both figures corresponds to an optical path of 520m (return way)

#### 4.3.5 Image motion and lateral pupil motion due to internal turbulence

The amount of image and lateral pupil motion introduced by internal air turbulence are two important parameters for the design of the PRIMA metrology system. These parameters need to be independently characterized to possibly evaluate how the metrology beams will overlap on the beam combiner.

Two light sources were used to measure independently the tilt (i.e image motion) and the lateral motion (i.e pupil motion) after propagation through the VLTI. These light sources were successively re-imaged on a CCD located in the interferometric laboratory.

In a first step, a  $\lambda=790$  nm point source was positioned in an image plane of the VLTI optical system, located in the VLTI laboratory. After beam collimation, and a round trip up to UT3, we observed the image motion of this light source. In this way, we deduced that the maximum radial tilt error introduced by internal air turbulence over 72 min corresponded to an angle of 100 marcsec on the sky.

In a second step, we observed with the CCD a red LED located at the center of the secondary mirror of a Unit Telescope. Since the secondary mirror is the “Stop” of the VLTI optical system, the CCD plane corresponded to an exit pupil plane. In this configuration, we monitored solely the impact of air turbulence on the lateral beam motion, which reached a peak value of 200  $\mu\text{m}$  over 30 min.

These results indicate that depending on the position of the re-combiner with respect to the exit pupil of the VLTI as well as on the selected beam diameter of the metrology system, we have to consider the implementation of a low frequency pupil and image tracker to enable long measurement sequence with PRIMA without degradation of the performance. This includes the possibility to operate with a minimum laser power thus reducing the straylight on the science detector.

## 5. CONCLUSION

This paper has presented some experimental results demonstrating that the combination of the phase meter and of the heterodyne assembly of the PRIMA metrology prototype is compatible with a nanometer accuracy level. The PRIMA metrology prototype has been successfully operated at Paranal over a path of up to 520 m. During this test campaign, we characterized the behaviour of the metrology system under representative operating conditions. We identified additional sources of errors related to the injection of the metrology beams into the stellar path, to the VLTI optical train and to the internal environmental conditions. Based on these results, we will refine our design and implement an absolute laser frequency stabilization.

## 6. ACKNOWLEDGMENT

This work is supported by the FINES program of the Swiss National Foundation. The authors would like to thank Marcel Groccia for his major contribution to the electronic design of the phase-meter.

## REFERENCES

1. F. Paresce et al., "Scientific Objectives of ESO's PRIMA facility", *these proceedings*
2. Y. Salvadé, R. Dändliker, S. Lévêque, "Superheterodyne Laser Metrology for the Very Large Telescope Interferometer", *ODIMAP III, 3rd topical meeting on Optoelectronics, Distance / Displacement Measurements and Applications*, University of Pavia, 20-22/09/01
3. S. Dubovitsky et al., "Metrology source for high resolution heterodyne Interferometer laser gauges", *Astronomical Interferometry*, R. D. Reasenberg, Eds., Proc. SPIE Vol. **3350**, Part Two, p.973, 1998
4. A. Arie et al., "Iodine spectroscopy and absolute frequency stabilization with the second-harmonic of the 1319 nm Nd:YAG laser", *Opt. Lett.* 18,p.1757,1993.
5. P. Halverson et al., "Techniques for the reduction of cyclic errors in laser metrology gauges for the space interferometry mission", *ASPE annual meeting*, Crystal City, Virginia, 2001